Effect of the Chemical Characteristics of Mesoporous Silica MCM-41 on Morphological, Thermal, and Rheological Properties of Composites Based on Polystyrene

León D. Pérez,[1,2] Juan F. López,[1] Víctor H. Orozco,[1] Thein Kyu,[2] Betty L. López[1]

[1]*Grupo Ciencia de los Materiales, Instituto de Química, Universidad de Antioquia, Sede de Investigación Universitaria (SIU), Calle 62 52-59 Medellín, Antioquia, Colombia*
[2]*Department of Polymer Engineering, University of Akron, Akron, Ohio*

Received 7 May 2008; accepted 12 August 2008
DOI 10.1002/app.29245
Published online 12 November 2008 in Wiley InterScience (www.interscience.wiley.com).

ABSTRACT: Mesoporous silica nanoparticles (MCM-41) with an average diameter of ~ 20 nm were synthesized by a sol-gel method using binary surfactant system. Polystyrene (PS) composites containing mesoporous silica nanoparticles were prepared by *in situ* polymerization of styrene monomers. Similar *in situ* polymerized PS composites were prepared based on the modified silica functionalized with methyl and vinyl groups. The effects of silylation on thermal and rheological properties of the PS/silica composites are investigated. Of particular importance is that the *in situ* polymerization of monomers within the mesoporous silica may trap some polymer chains, if not all, thereby affording a greater physical interaction between polymer and the porous fillers, whereas the chemical modification of silica surface promotes the polymer–filler interaction, which in turn enhances the thermal stability of composites. © 2008 Wiley Periodicals, Inc. J Appl Polym Sci 111: 2229–2237, 2009

Key words: polymer nanocomposites; mesoporous silica; polystyrene

INTRODUCTION

A conventional wisdom in filled polymer composites is to achieve the highest performance at the lowest filler loading. To attain such filled composites, the filler–polymer interactions and the filler dispersion are among many factors that have been hitherto widely investigated.[1–6] By virtue of the chemical nature of the complementary groups such as acid and base groups, the filler–polymer interaction can be enhanced, which in turn promotes the adsorption of polymeric chains onto the filler surface. Alternatively, the filler surfaces may be modified by a direct deposition of a polymer layer onto the mineral fillers via *in situ* polymerization. For instance, as demonstrated by Kyu et al.,[7] *in situ* ring-opening polymerization of caprolactam directly onto the colloidal kaolin fillers has led to enhanced wetting properties of the kaolin surface. Subsequent mixing of these colloidal fillers with conventional polyamides further yields the improved mechanical properties of the polyamide/kaolin composites.

Correspondence to: L. D. Pérez (ldperez@udea.edu.co).
Contract grant sponsors: Universidad de Antioquia and COLCIENCIAS (Colombia) through the program; Apoyo a la comunidad científica nacional a través de becas doctorales.

Journal of Applied Polymer Science, Vol. 111, 2229–2237 (2009)

Filler dispersion can be influenced by filler–polymer interactions, i.e., better filler dispersion can be obtained by either promoting filler–polymer interaction or lessening the filler-filler interactions. Surface modification of filler particles have been attempted via silylation of the silica and dehydration at elevated temperatures. However, although the modification of the filler surface with non polar groups such as alkyl chains often induces particle dispersion, lower filler–polymer interactions can be obtained.[8]

To simultaneously improve the filler–polymer interaction and the filler dispersion, the filler surface may be grafted with functional groups such as vinyl[9] and sulfur,[10,11] which are capable of reacting or interacting with the polymer matrix. Over the years, the utilization of fillers with tailored surfaces, like mesoporous silica, has increased,[9,12–19] because of their larger surface area afforded by these mesopores relative to the conventional fillers. These composites may be prepared more effectively by *in situ* polymerization, because the liquid monomer is less viscous and easier to diffuse into these structural pores of the fillers when compared with the more viscous giant macromolecular chains.[9,16] Moreover, the *in situ* polymerized chains confined within these mesopores further promote the filler–polymer interactions and the filler dispersion at the same time.

Several properties are expected to increase by mineral reinforcement to polymer matrix. The

thermal stability has been of immense interest to many researchers, because in case of fire the pyrolysis of some polymers produces toxic gases, which could be hazardous to human health. Such problem may be overcome based on the combination of various properties such as the filler's ability of catching free radicals, the improved barrier properties of the mineral filled composite, and the suppression of the pyrolysis rate due to the reduced chain mobility. The present work is focused on the characterization of the interactions between polystyrene (PS) and mesoporous silica and the effect of the chemical characteristics of the silica on the thermal, rheological, and morphological properties of the composites.

EXPERIMENTAL

Materials

Silica source used in this study was tetraethoxysilane (TEOS) with 98% purity. The cationic surfactant, cetyltrimethylammonium bromide (CTAB with 99% purity), and the silylation agent, trimethylchlorosilane (TMCS with 98% purity), were purchased from Acros Organics (Geel, Belgium). Nonionic surfactant triblock copolymer ($EO_{106}PO_{70}EO_{106}$) Pluronic F-127, styrene monomer, and the functionalization agent, triethoxyvinylsilane (TEVS, 97% purity), were purchased from Sigma-Aldrich (St. Louis, MO). Free radical initiator, i.e., 2,2′-azobis-isobutyronitrile (AIBN), was supplied by Akzo Novel (Chicago, IL). Analytical grade toluene and acetone were purchased from Merck (Bogotá, Columbia). The styrene monomer was distilled under reduced pressure at 135°C and the AIBN was recrystallized from a mixture of methanol/water. Other chemicals were used as received.

Sample preparation

Synthesis of mesoporous materials

The molar reagent ratio used in the synthesis of the mesoporous silica (MCM-41) by the sol-gel method was 1 TEOS : 0.424 CTAB : 0.00945 Pluronic F-127 : 99.05 H_2O : 5.09 NH_4OH. The cationic surfactant (CTAB) was used as a template for the porous structure. The nonionic cosurfactant (Pluronic F-127) was utilized to stabilize the colloidal particles and avoid their aggregation. In a typical synthesis scheme, 2.6 g of CTAB and 2.0 g of Pluronic F-127 were dissolved under rigorous stirring in 30 mL of hydrochloric acid solution (pH = 0.5), followed by dropwise addition of 3.5 g of TEOS at room temperature until a clear solution was obtained. Then, 3.0 mL of ammonium hydroxide solution at 28 wt % was added. The obtained white gel was maintained under continuous stirring for 24 h. Finally, the resulting gel was dried at 60°C in air for 1 week, followed by calcination at 600°C to eliminate the surfactants. The temperature was increased from room temperature to 600°C at 1.5°C/min.

Mesoporous silica functionalization

Mesoporous silica was functionalized by a postsynthesis grafting method. The samples were degassed under reduced pressure at 150°C for 3 h. The silylation reactions were carried out using stoichiometric amounts of the organosilane reagents (TMCS and TEVS) and toluene as a solvent, and the reaction was carried out at 50°C for 24 h. For the reaction with TMCS, triethylamine in the catalytic amount was added to the reaction mixture to improve the yield. Finally, the silylated silica from each one of the reactions was collected by filtration and thoroughly washed with toluene, followed by ethanol and finally by deionized water; then the materials were dried at 25°C.

Synthesis of nanocomposites

The PS/mesoporous silica composites were synthesized by *in situ* bulk polymerization of the styrene in the presence of silica, using AIBN at 0.25 wt % as a free radical initiator with respect to the monomer amount. The mixture of styrene, silica, and initiator was carefully homogenized and kept under stirring for 1 h at ambient temperature. The styrene was polymerized at 67°C under magnetic stirring in inert atmosphere for 48 h; then the temperature was raised to 125°C and kept for 24 h in N_2 to cure the polymer and to induce the complexion of all the radical reactions; in the case of the composite containing vinyl modified silica, it is expected that this final heating stage promotes the reaction of PS chains with the vinyl groups if they did not react during the initial step. Finally, the pressure was reduced and the samples were kept for another 24 h at the same temperature to eliminate residual monomer, if any.

Regarding the unmodified silica, three different concentrations were used, viz., 5, 10, and 15 wt %. The samples were designated as PS5, PS10, and PS15, respectively. The silica modified with TMCS and TEVS were used at 15 wt %; these samples were designated as PS15M and PS15V, respectively. Neat PS without silica was used as a reference.

Sample characterization

Pore size distribution, surface area, and porous volume were determined with a nitrogen adsorptometer (ASAP 2010; Micromeritics); the measurements were carried out at −196°C. The surface area was calculated using the Brunauer–Emmett–Teller (BET) model, whereas the pore size distribution was

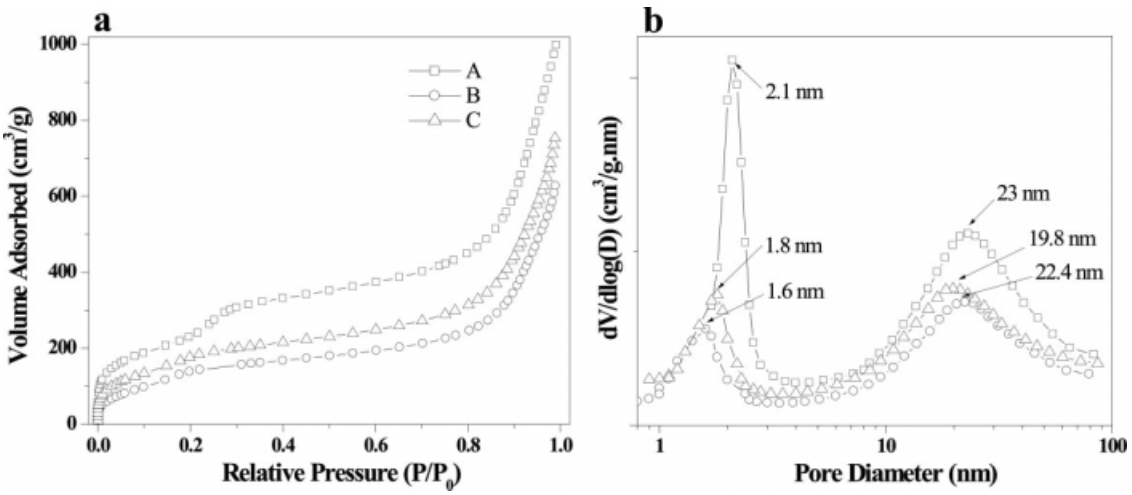

Figure 1 Nitrogen adsorption characterization of unmodified (A), trimethyl (B), and vinyl (C) functionalized mesoporous silica: (a) adsorption isotherms; (b) pore size distribution plots.

evaluated in accordance with the Barret–Joyner–Halenda (BJH) approach.

The infrared spectra of the silica were obtained using a diffuse reflectance accessory in a FTIR spectrometer (Spectrum One; Perkin-Elmer). The FTIR spectrum thus acquired is the average of 64 scans.

The decomposition temperatures of silica and its PS composites were determined by thermogravimetric analysis (TGA) using a TG analyzer (Q500; TA Instruments). The heating rate of 10°C/min was employed in the temperature range from 30 to 600°C in air.

The molecular weight (M_w) and polydispersity of PS in the composites were determined by gel permeation chromatography. The composites were extracted with tetrahydrofuran under sonication and then filtered to remove the silica residuals. The analyses were carried out using a HPLC waters equipped with a refraction index detector.

The morphological features of these composites were examined by scanning electron microscopy (SEM) in a FEI/Phillips XL30. The specimen was fractured and subsequently shadowed the fractured surface with gold under vacuum.

The mesoporous silica particles were examined by transmission electron microscopy (TEM) using a Phillips CM20. The sample powders were dispersed in propanol under sonication, and then an aliquot was put on a cupper grid and the solvent was evaporated under vacuum.

The glass transitions of the PS/silica composites were measured by differential scanning calorimetry in a calorimeter (Q100; TA Instruments). Samples were heated at 30°C/min from room temperature to 180°C and kept for 5 min to erase thermal history, if any, and subsequently cooled down to ambient temperature at 30°C/min. Finally, the DSC thermograms were collected at a heating rate of 10°C/min from ambient to 180°C.

The reversible heat capacity of the PS/silica composites was determined by modulated temperature differential scanning calorimetry (MTDSC) by using the heating module integrated into the calorimeter (Q100; TA Instruments). The samples were heated at 30°C/min until 180°C and held for 10 min and then cooled down at 30°C/min to −10°C. Finally, the MTDSC were acquired by heating at 3°C/min up to 180°C; the temperature was modulated at ±1°C/min.

Rheological tests were conducted using a rotational rheometer (ARES; TA Instruments). The dependence of the shear modulus (G') on the shear strain was measured at a frequency of 10 Hz and at 200°C.

RESULTS AND DISCUSSION

Mesoporous silica characterization

Nitrogen adsorption measurement

Figure 1(a) shows the nitrogen adsorption isotherm of the typical for silica (MCM-41) in comparison with TMCS and TEVS modified mesoporous silica. From Figure 1(a), it was found that the adsorbed volume of nitrogen by the silylated mesoporous silica is reduced, implying that the size of the pores decreased because of the incorporation of the organic groups within these pores. In all samples, the adsorbed volume increases drastically at the relative pressure of unity; this is due to the interparticle pores that are formed by agglomeration of the nanoparticles. The corresponding Figure 1(b) shows the pore size distributions for unmodified and modified silica, showing two types of porosity. The first one is

TABLE I
Porous Characteristics of the Mesoporous Silica Nanoparticles

Sample	Specific surface area (m^2/g)	Specific pore volume (cm^3/g)
MCM-41	833 ± 9	1.39
MCM-41 TEVS	639 ± 9	1.08
MCM-41 TMCS	504 ± 11	0.88

of the order of 2 nm, which is a characteristic size of the mesopores of the as-prepared silica by using CTAB as a template. The second appears around 23 nm, which may be attributed to the interparticle pores generated by the agglomeration of the particles [Fig. 1(b)]. Upon modification of mesoporous silica particles with trimethyl and vinyl groups, both the intraparticle and the interparticle pores reveal the reduction in their sizes, suggesting that these organic modifiers indeed enter into the primary pores as well as into the interparticle regions. The surface area and specific pore volume of the as-prepared and silylated silica samples are tabulated in Table I. Surface areas were calculated with a minimum correlation coefficient of 0.9972. It is seen that both surface area and specific pore volume decline upon functionalization in the sequence of TEVS and TMCS modifications.

Transmission electron microscopy

Figure 2 shows the TEM image for the mesoporous silica, showing numerous tiny particles in the form of agglomerates. The diameter for the individual (primary) particles is ~ 20 nm. In the enlarged view (upper left), the hexagonal arrangement of the pores can be discerned within the primary particles, which are typical characteristic for this kind of porous silica.

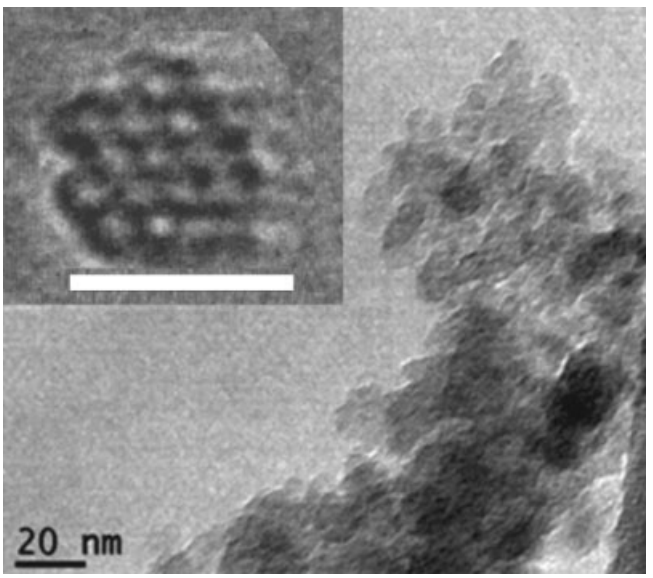

Figure 2 TEM image of the mesoporous silica MCM-41.

Infrared spectroscopy

Figure 3 shows the FTIR spectra of the as-prepared and functionalized mesoporous silica. The as-prepared silica shows the characteristic absorption bands for these materials such as O—H stretching and bending at 3463 and 1640 cm^{-1}, respectively, and Si—O stretching at 1079 cm^{-1}. No peaks associated with organic groups are present in the as-prepared silica.

Vinyl functionalized mesoporous silica reveals a weak shoulder at 3074 cm^{-1} that corresponds to alkenes C—H stretching mode and a band at 1608 cm^{-1} which is characteristic of the C=C stretching vibration, indicative of the vinyl groups. In the trimethyl functionalized silica, the typical bands for alkyl C—H stretching at 2961 and 2856 cm^{-1} are evident, which confirms the presence of those methyl organic groups in the material.

Thermogravimetric analysis

According to TGA and their corresponding derivative thermograms, shown in Figure 4(a), the as-prepared silica shows little or no degradation up to 700°C (i.e., less than 2 wt %). The slight weight loss may be due to desorption of chemisorbed water and the silanol present in the neat silica. In the silylated silica, two-step drops in the weight loss curves can be seen. This trend is more evident in the

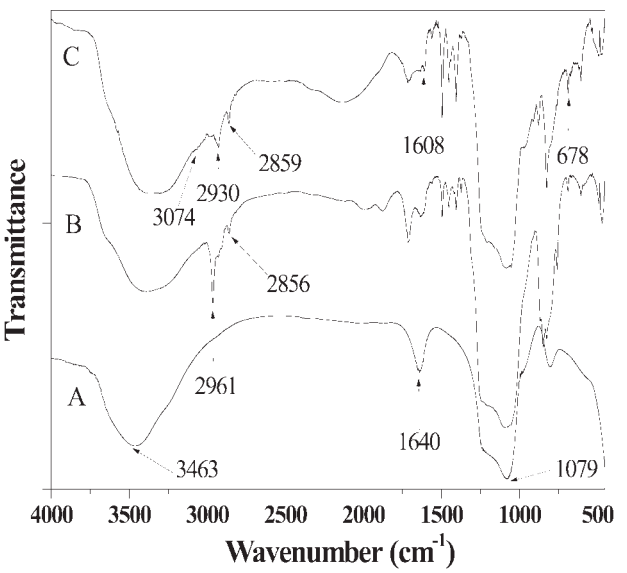

Figure 3 FTIR spectra of the unmodified (A), trimethyl (B), and vinyl (C) silylated mesoporous silicas.

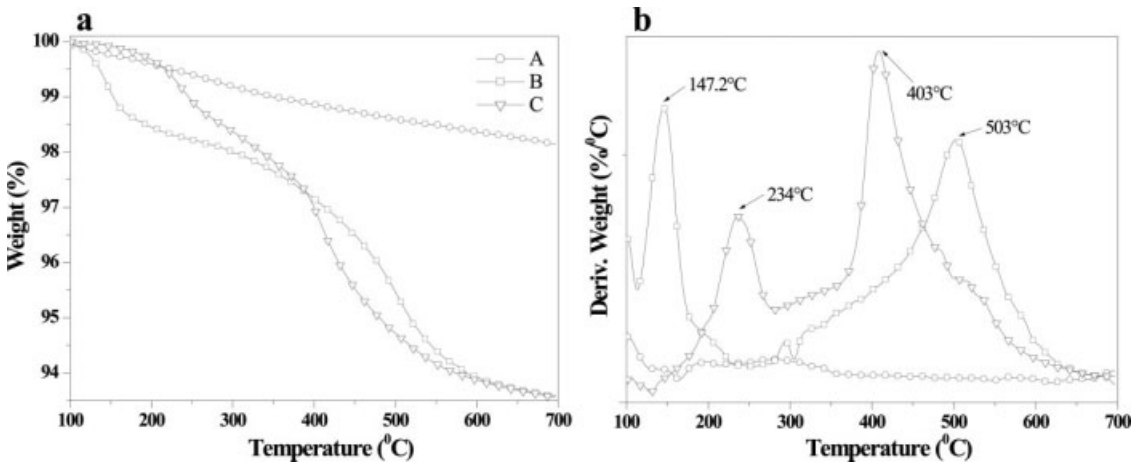

Figure 4 (a) Thermogravimetric analysis of the unmodified (A), trimethyl (B), and vinyl (C) silylated mesoporous silica MCM-41 and (b) derivative weight loss.

corresponding derivative weight loss versus temperature curves [Fig. 4(b)]. In the silica modified with TMCS, the first derivative peak appears at 147°C which may be attributed to evaporation of the silane monomers and dimers adsorbed at the silica surface. These unbound organics are not completely extracted during repeated washing. The same trend can be witnessed in the TEVS modified silica, except that the peak appears at a higher temperature of 234°C, suggesting that unbound triethoxyvinylsilane escapes later relative to the trimethyl modifier. This trend reverses in the second derivative weight loss peaks which are located at 503°C for the trimethyl modified silica and 403°C for the degradation of the vinyl modifier, implying that the bound vinyl modifier on the silica is less thermally stable as compared to the bound trimethyl groups.

Composites characterization

Molecular weight and polydispersity

Table II presents the molecular weight and polydispersity of the PS reference and the PS in the composites. The molecular weight increases with the addition of silica, which can be due to the stabilization of the propagating radicals afforded by the mesoporous silica during the polymerization of the styrene. On the other hand, the higher polydispersity of the PS in the composites compared with the reference is attributed to the increase in the viscosity due to the presence of silica particles.

Scanning electron microscopy

The morphology of the composites containing 15 wt % of unmodified silica and the corresponding composites with methyl and vinyl silylated silicas was analyzed using SEM. Figure 5 shows the respective images of their cross sections and their surfaces.

The composite containing 15 wt % of unmodified silica, shown in Figure 5(a), presents a smooth surface and some large agglomerates (around 1 μm), indicating poor dispersion of the silica. The cross section [Fig. 5(b)] also reveals some agglomerates, and it is seen that the silica particles are imbibed in the matrix and wetted by the polymer.

In the case of composite containing methyl silylated silica [Fig. 5(c)] the surface is rough, and smaller loose agglomerates are observed. The cross section [Fig. 5(d)] shows better dispersion compared with the previous composite, but the particles seem to be segregated from the polymeric matrix.

The composite containing vinyl silylated silica presents a smooth surface; the silica particles appear well dispersed and imbibed in the matrix [Fig. 5(e)]. The cross section image [Fig. 5(f)] shows that the filler is well wetted by the polymer. Isolated particles can be seen.

As explained earlier the presence of polar groups on the silica surface induces agglomeration because the interaction silica–silica prevails on PS–silica interactions. On the other hand, silanol groups allow electron donor–acceptor interactions with phenyl

TABLE II
Molecular Weight and Polydispersity for the PS in the Composites Containing Different Amounts of Unmodified Silica and 15 wt % of Silica Modified with Methyl and Vinyl Groups

Composite	M_w ($\times 10^5$)	M_w/M_n
PS	1.7	2.4
PS5	3.5	2.9
PS10	3.2	2.8
PS15	4.6	2.9
PS15M	3.3	3.0
PS15V	2.5	3.0

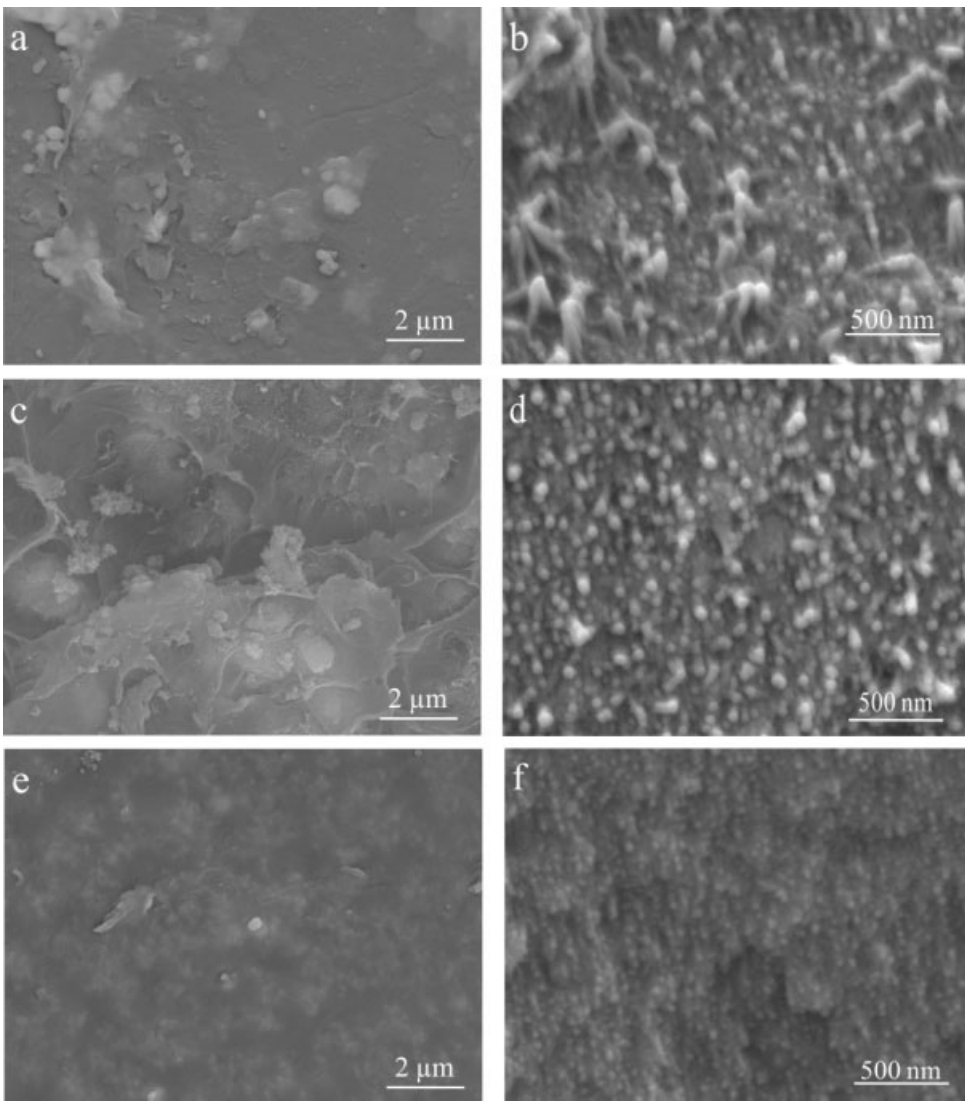

Figure 5 SEM images of the composites, surface (left) and cross section (right): (a, b) PS15; (c, d) PS15M; (e, f) PS15V.

groups on the polymer, which are responsible for the wetting of the particles by polymer.

Modification of the silica with methyl groups induces better dispersion of the particles compared with the unmodified silica because of the reduction of silanol content, and as a consequence, the wetting of the filler by the PS chains is lessened because the electron donor–acceptor interactions decreased too.

When the silica particles are modified with vinyl groups the reduction of silanol groups is accomplished by the formation of silica–polymer covalent bonds during the *in situ* polymerization of PS, resulting in a significant improvement on dispersion and higher silica–PS interaction.

Rheology test

Figure 6(a) illustrates the shear elastic modulus (G') as a function of shear strain (%). The neat PS shows the invariant G' versus shear strain behavior, which is characteristic of linear viscoelastic behavior of nonfilled polymers. However, with the addition of unmodified silica of 5, 10, and 15 wt %, the magnitude of G' increases dramatically with the filler loading. Concurrently, there appears an appreciable drop in G' with increasing strain, especially in the high shear strain region. Such nonlinear behavior of the G' versus shear strain may be attributed to the breakdown of filler–filler network known as Payne effect.[20] This trend is less pronounced in the PS5 composite, because the concentration of the silica is probably not enough to establish a strong filler–filler network across the polymer matrix.

Figure 6(b) demonstrates the effect of silylation of silica with TMCS and TEVS on the composite behavior of PS at the loading level of 15 wt % of silica. At low strain %, the G' value is relatively high for the unmodified PS15 composite. Upon functionalization

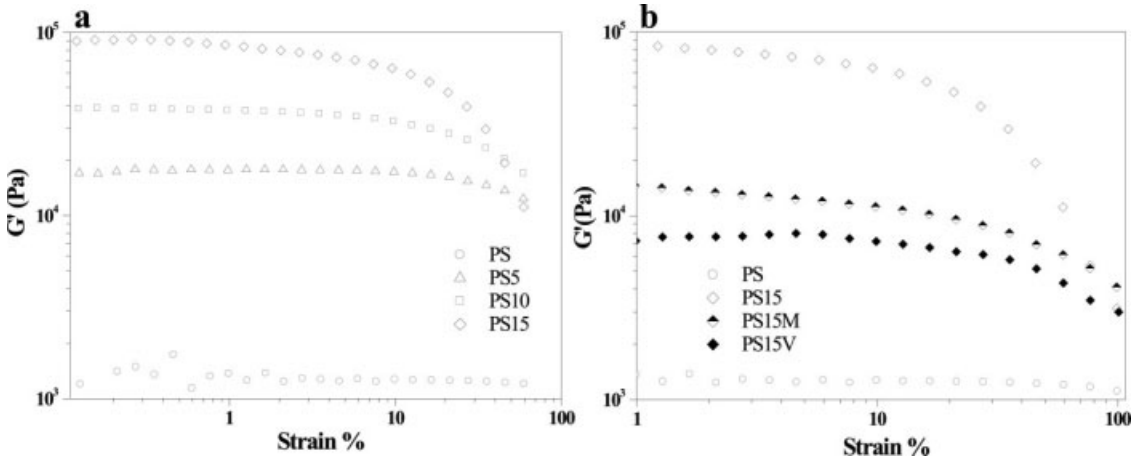

Figure 6 Dependence of the shear elastic modulus on the shear strain %: (a) Effect of the amount of unmodified silica on the rheological properties; (b) Effect of the silylation on the rheological properties.

of the silica, the G' value drops noticeably for both the PS15M and PS15V composites. The decreasing trend of G' with strain becomes subtle the PS15M composite, which may be a consequence of the reduction in the silica–silica interactions. This plasticization effect is even more noticeable in the case of PS15V composite, which can be due to the wrapping of the silica particles by PS chains, thereby reducing the interparticle interactions. It may be hypothesized that vinyl groups of the mesoporous silica surface may be involved in the *in situ* free radical polymerization of PS in the PS15V composite so that the PS chains may be attached more readily on the vinyl silylated silica than its PS15M counterpart, thereby rendering more pronounced plasticization.

Differential scanning calorimetry

Table III shows the variation of T_g with silica loading as determined by conventional DSC for the unmodified and modified composites. The glass transition of the PS increases with the addition of unmodified silica; a significant increase in T_g is seen above 10 wt %. This finding of the matrix T_g enhancement may be attributed to the reinforcement effect afforded by the filler. The drastic increase in the T_g is consistent with the formation of the silica–PS network suggested in the rheological measurement. In the case of functionalized composites such as PS15M, the T_g of PS was found to be lower than the corresponding unmodified silica composite. The lowering of T_g by the functionalization of the mesoporous silica may be attributed to the plasticization effect caused by the trimethyl groups grafted on the silicate filler interface.[6] The highest mobility of the plasticized PS chains in turn facilitates better filler dispersion which is good accord with the reduction in the G' value with functionalization of silica. Besides this effect, modification with TMCS also reduced the concentration of silanol groups and therefore the strength of the interactions between the silica and PS chains also declined; as mentioned earlier, these specific interactions take place between silanol groups on the silica and phenyl groups on the PS.

It may be envisaged that there are two kinds of interactions competing with each other, viz., chemical and physical interactions between the filler and the polymer matrix. Chemical interaction such as electron donor–acceptor is highly unlikely to occur between styrene and the silica grafted with silanol groups, except that in the vinyl group of the PS15V composite it might involve in the *in situ* free radical polymerization of PS. In the trimethyl grafted silica composite (PS15M), the occurrence of chemical interaction is more remote.

In the *in situ* polymerization of styrene in the presence of unfunctionalized silica, some styrene monomers probably diffuse into both within the primary pores and the interparticle porous regions by virtue of the mesoporous nature of the silica utilized. This *in situ* polymerization of styrene affords the direct deposition of PS chains on the silica porous interfaces/surfaces. The *in situ* polymerized chains confined inside the silica pores and their interparticle

TABLE III
Thermal Behavior of the PS/Silica Composites Measured by DSC and TGA

Sample	DSC analysis T_g	TG analysis	
		Onset (°C)	Maximum (°C)
PS	91.4	304.7	338.9
PS5	94.5	324.1	375.3
PS10	105.9	355.6	380.3
PS15	103.3	367.0	389.4
PS15M	99.3	367.8	384.3
PS15V	89.2	371.9	399.5

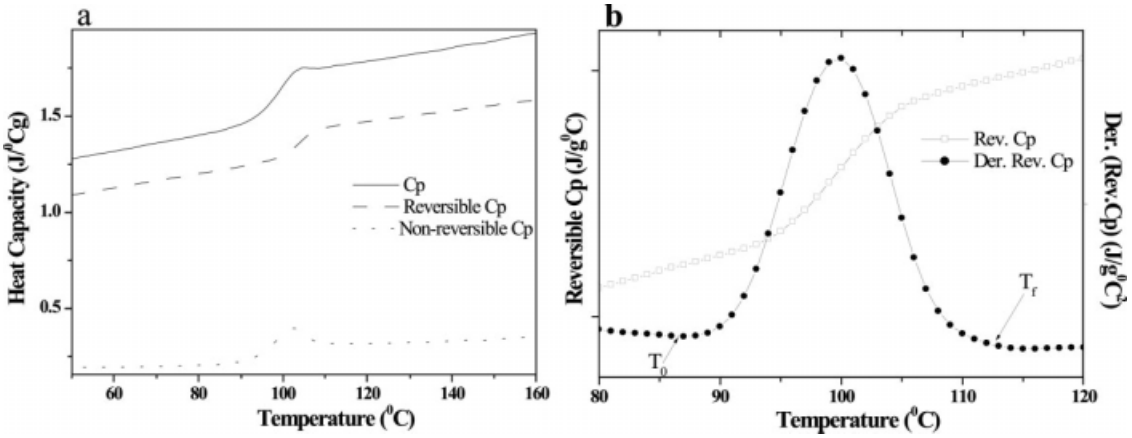

Figure 7 (a) Typical MTDSC thermogram for the PS composites and (b) derivative of the reversible heat capacity.

regions created by the agglomeration would promote the physical interactions between the matrix chains with the unfunctionalized silica. In the case of the composite containing the modified silica silylated with TMCS, the interaction between the silica and the PS chains can be reduced when compared with the corresponding composite with unmodified silica, which may be attributed to the plasticization effect by the organic modifier. In the PS15V composite, the T_g for the PS was not improved by the modification, except that a better dispersion of silica was seen in the composite. This behavior may be attributed to the plasticization by the chains bonded to the surface. Needless to say, any residual amount of unbounded silane can also act as a plasticizer.

Thermogravimetric analysis

The overall TGA results comparing the thermal stability of the PS composites as a function of filler loading are summarized in Table III. As expected, the thermal stability of the composites prepared with the unmodified silica increases with increasing filler amount. The modification with methyl groups shows no improvement in onset of the degradation; however, the temperature of the maximum degradation moved to a lower value relative to the unmodified silica at the same loading level. The improvement on the thermal stability is related to the extent of the silica–PS interactions. The modification of silica with methyl groups, which do not present specific interactions with PS, reduces the silanol content, resulting in a decrease of the thermal stability in comparison to the unmodified filler.

A significant improvement in the thermal stability was obtained for the vinyl modified silica composites which could result from the finer dispersion of the silica as well as the formation of silica–PS covalent bonds.

Modulated temperature differential scanning calorimetry

To have a more detailed insight into the morphology of the composites, MTDSC was used to calculate the amount of immobilized polymer by the filler. The polymer chains anchored on the filler surface may not represent the glass transition temperature of the bulk because their mobility is more restricted at the surface.

Figure 7(a) shows a typical MTDSC thermogram of the PS that permits the determination of a total thermogram and two separated thermograms in the same experiment, associated with the reversible and nonreversible phenomena, respectively. In the present calculation, the reversible specific heat capacity (C_p) signal was used; hereafter, C_p refers to reversible C_p.

The reduction in ΔC_p at the glass transition temperature of the composites relative to the pure polymer from MTDSC can be quantitatively related to the amount of immobilized polymer by the filler or a crystal as in the case of semicrystalline polymers.[21] This conjecture can be confirmed by the reduction of the intensity of tan δ in the dynamic mechanical experiments as reported earlier.[22,23]

Because of the small values of ΔC_p at T_g, a more accurate measure can be achieved by calculating the area under the derivative reversible C_p versus temperature curve as shown in eq. (1) as well as in Figure 7(b).

$$\Delta C_{p,\mathrm{rev}} = \int_{T_0}^{T_f} dC_{p,\mathrm{rev}}\, dT \tag{1}$$

The amount of immobilized polymer by the filler can be computed as follows:

$$\text{Adsorbed PS (wt\%)} = \left(1 - \frac{100}{100 - \%\ \text{filler}} \times \frac{\Delta C_{p\mathrm{composite}}}{\Delta C_{p\mathrm{PS}}}\right) \times 100\% \tag{2}$$

TABLE IV
MTDSC Results: Immobilized Polymer Amounts of Different Composites

Sample	ΔC_p at T_g [J/(g °C)]	Filler amount (wt %)[a]	PS immobilized by the filler (%)
PS	0.140	–	–
PS15	0.102	13.8	15.2
PS15M	0.106	13.5	12.8
PS15V	0.110	13.3	9.5

[a] Calculated from the TGA experiments.

where % filler is the percentage of filler in the composite, $\Delta C_{p\ \text{composite}}$ and $\Delta C_{p\ \text{PS}}$ are the heat capacity change at T_g of the composite and the pure PS, respectively.

Table IV shows the calculated results for the composites containing 15 wt % of silica. The largest amount of immobilized polymer was found for the unmodified silica, suggesting that the physical interaction is dominant. The lowest immobilized polymer was found for the case of silica modified with TEVS. There are two possible scenarios to account for this finding: i.e., the vinyl group on the silica pore would promote covalent bonding between the silica and the PS chains because vinyl can copolymerize with styrene during *in situ* polymerization. Hence, the motion of the trapped or anchored PS within these primary pores will be restricted and thus will be immobilized. On the other hand, the vinyl group on the silica particle surface could contribute to plasticization effect, thereby lowering the T_g as well as the viscosity and thus affording better filler dispersion; however, the strength of the filler silica–silica is decreased because of reduction of the silanol content and hindrance originated by the chains anchoring the filler surface.

In contrast to the report by Sargsyan et al.[23] for the PS composites filled with silicon dioxide nanoparticles, the present PS/mesoporous silica (unmodified MCM-41) composites revealed that a considerable amount of polymer was immobilized, even though a lower concentration of silica utilized. This finding may be attributed to the mesoporous characteristics of the silica filler utilized such that PS chains can grow inside the mesopores as well as on the silica surface (or interface region) during the *in situ* polymerization.

CONCLUSIONS

In summary, we have demonstrated the effect of filler loading on thermal stability, dynamic mechanical properties, and glass transition temperatures of the *in situ* polymerized PS/MCM-41 composites. Of particular importance is that the *in situ* polymerization of styrene on the mesoporous silica has led to the improved G', enhanced glass transition, as well as increased immobilized polymer amount. Upon modification of these silica nanoparticles with trimethyl and vinyl functional groups, the T_g of the composites as well as dynamic modulus decrease when compared with the unmodified silica filled composites. The lower viscosity of the PS/modified silica composites improves their melt processability, which in turn affords finer silica dispersion. The thermal stability for PS-unmodified mesoporous silica composite is improved by increasing the amount of silica and by the establishment of silica–PS covalent bond in the case of the composite containing silica grafted with vinyl groups, but the modification with methyl groups shows little improvement of the degradation temperature.

References

1. Schaefer, D. W.; Justice, R. S. Macromolecules 2007, 40, 8501.
2. Mills, S. L.; Lees, G. C.; Liauw, C. M.; Rothon, R. N.; Lynch, S. J Macromol Sci Phys 2005, 44B, 1137.
3. Burya, O. I.; Kozlov, H. V.; Lipatov, Y. S. Mater Sci 2003, 39, 758.
4. Karasek, L.; Sumita, M. J Mater Sci 1996, 31, 281.
5. Edwards, D. C. J Mater Sci 1990, 25, 4175.
6. Jordan, J.; Jacob, K. I.; Tannenbaum, R.; Sharaf, M. A.; Jasiuk, I. Mater Sci Eng A 2005, 393, 1.
7. Kyu, T.; Zhu, G. C.; Zhou, Z. L.; Tajuddin, Y.; Qutubuddin, S. J Polym Sci Part B: Polym Phys 1996, 34, 1769.
8. Milczewska, K.; Voelkel, A. J Chromatogr A 2002, 969, 255.
9. He, J.; Shen, Y.; Yang, J.; Evans, D. G.; Duan, X. Chem Mater 2003, 15, 3894.
10. Choi, S. S.; Kim, I. S.; Woo, C. S. J Appl Polym Sci 2007, 106, 2753.
11. Zhou, M.; Song, Y.; Sun, J.; He, L.; Tan, H.; Zheng, Q. Acta Polym Sin 2007, 153.
12. He, J.; Shen, Y.; Evans, D. G. Microporous Mesoporous Mater 2008, 109, 73.
13. He, J.; Shen, Y.; Evans, D. G.; Duan, X. Compos Part A: Appl Sci Manuf 2006, 37, 379.
14. Ji, X.; Hampsey, J. E.; Hu, Q.; He, J.; Yang, Z.; Lu, Y. Chem Mater 2003, 15, 3656.
15. Moller, K.; Bein, T.; Fischer, R. X. Chem Mater 1998, 10, 1841.
16. Pérez, L. D.; Giraldo, L. F.; Brostow, W.; López, B. L. e-Polymer 2007, 29, 1.
17. Wang, N.; Li, M.; Zhang, J. Mater Lett 2005, 59, 2685.
18. Perez, L. D.; Giraldo, L. F.; Lopez, B. L.; Hess, M. Macromol Symp 2006, 245/246, 628.
19. Lopez, B. L.; Perez, L. D.; Mesa, M.; Sierra, L.; Devaux, E.; Camargo, M.; Campagne, C.; Giraud, S. e-Polymer 2005, 18, 1.
20. Cassagnau, P. Polymer 2003, 44, 2455.
21. Wunderlich, B. Prog Polym Sci (Oxford) 2003, 28, 383.
22. Arrighi, V.; McEwen, I. J.; Qian, H.; Prieto, M. B. S. Polymer 2003, 44, 6259.
23. Sargsyan, A.; Tonoyan, A.; Davtyan, S.; Schick, C. Eur Polym J 2007, 43, 3113.